



Proceedings
PRO 38

Testing and Modelling Chloride Ingress into Concrete

Proceedings of the
3rd International RILEM Workshop

Edited by C. Andrade and J. Kropp

RILEM Publications S.A.R.L.

CHLORIDE DIFFUSION AND THE INFLUENCE OF THE SATURATION DEGREE OF THE CONCRETE

A. T. C. Guimarães¹, P. R. L. Helene²

¹ University of Rio Grande, Materials and Construction Department
DMC/FURG, Brazil.

² University of São Paulo, Civil Construction Engineering Department
PCC/USP, Brazil.

Abstract

GUIMARÃES [1] have shown that the application of deterministic models based only on the Fick's Laws can exhibit considerable differences to the effective chloride profiles in existing marine structures. In this research, a laboratory test method to estimate the influence of the concrete saturation degree (SD) on chloride diffusion was developed. Test results were applied to an existing 22 years old marine structure. Results indicate that the concrete SD has a great influence on chloride diffusion and requires further research. Therefore, this factor should be taken into account when estimating the service life of concrete structures.

1. Introduction

When one tries to relate penetration profiles of chlorides in long-service-life structures (above 20 years) using deterministic models based only on the Fick's Law we can find differences between the penetration depth observed in reality and the predicted depth. According to GUIMARÃES [1] recent studies have shown large differences between the chloride penetration depth foreseen by deterministic models and the effective values found in marine piers in the South of Brazil. The concrete surfaces of these piers have a high chloride content (2% in relation to the cement mass). The research was done taking into account factors such as variations in compressive strength, seasonal temperature oscillations, cement type and water-cementitious materials ratio (w/cm) [1]. It should be highlighted that high values for chloride content were found both in the rainy (winter) and the dry (summer) seasons.

It is believed that the increased resistance to chloride penetration found in actual structures may be due to the fact that the equilibrium water content in the concrete is below the saturation level. This can generate differences between laboratory results and

existing concrete structures since laboratory tests for diffusion coefficients are carried out in saturated test specimens [2, 3, 4, 5].

Two test methods were developed to investigate the influence of this factor. The first determines the influence of the different saturation degrees (SD) on chloride diffusion. The second measures the variation of the SD in the concrete outermost layers in a marine environment. A 22-year-old marine pier was then tested using these methods.

2. Tests of diffusivity variation in relation to the saturation degree (SD) – laboratory tests

2.1. Materials

These tests were developed and carried out using test specimens prepared with cement paste. A high early strength Portland cement (equivalent to Type III – ASTM C 150 [6]) was used.

This cement was chosen because of its faster hydration characteristics in relation to other types of cement. Thus the influence of possible differences in cement hydration for the different moisture contents used during the test is reduced.

A paste with a 0.5 w/cm was prepared and 50 $\Phi 30 \times 45$ -mm cylindrical specimens were prepared in plastic molds. Five $\Phi 50 \times 100$ -mm cylindrical specimens were prepared in metallic molds for characterization tests (Fig. 1).

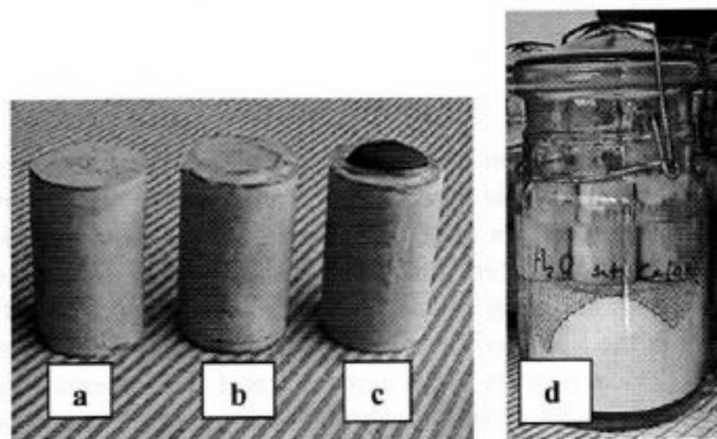


Figure 1. Test specimen preparation: a) cylindrical specimen with sand-papered top; b) cylindrical specimens with silicone ring; c) cylindrical specimens with contamination layer; d) cylindrical specimens of the 100 % SD group, partly immersed in a saturated solution of $\text{Ca}(\text{OH})_2$

Twenty-four hours after casting, the cylindrical specimens were removed from their molds and some millimeters were removed from the top by abrasion to eliminate the outer layer; and reduce the exudation effect (Fig. 1a). Following that, they were cured in a water tank for 14 days, and then stored in a laboratory environment to the age of 28 days. The $\Phi 50 \times 100$ -mm cylindrical specimens had a mean absorption of 29.7 % by mass, average specific mass of 1468 kg/m^3 (paste dry in an oven at $105 \pm 5 \text{ }^\circ\text{C}$ for 72 hours) [16] and an average compressive strength of 29 MPa after 28 days.

In order to estimate the dry mass of the $\Phi 30 \times 45$ -mm cylindrical specimens, 6 samples were selected at random from the 50 specimens available. These specimens were dried in an oven at $105 \pm 5 \text{ }^\circ\text{C}$ for 72 hours. Their average mass was 48.3 g, with a standard deviation of 0.58 g.

2.2. Test to estimate the influence of the saturation degree (SD)

A layer of cement paste with chlorides (NaCl 5% by cement mass) was applied to the top of the $\Phi 30 \times 45$ -mm cylindrical specimens. After moisture contents had stabilized, a chloride penetration profile was obtained by slicing half of the cylindrical specimens and by testing chloride ion concentrations in the paste. This initial profile could be produced by the penetration of chlorides by capillary absorption. After about 3 months, when the SD of the cylindrical specimens had stabilized, a second profile was obtained for each group of SD (4 groups of SDs in the range of 55%, 75%, 90% and 100%, Groups I, II, III and IV respectively, with 10 samples for each group). The analysis of the latter group provided the diffusion coefficient for each SD.

A silicone rubber ring was placed on the top of the cylindrical specimens to make application of the layer of chloride-contaminated paste with the same composition easier and to prevent spilling, which would have contaminated the lateral surface of the cylindrical specimens (Fig. 1b).

SDs in the range of 55%, 75% and 90% were obtained by natural drying or by wetting 28-day-old cylindrical specimens with distilled water. To keep the moisture of each group constant, the specimens in each group were placed in vacuum plastic bags. The 100% SD was obtained by partly immersing the cylindrical specimens to the height of 30 mm in a saturated solution of $\text{Ca}(\text{OH})_2$ (Fig. 1d). The SDs of samples were stabilized before and after the contamination with the chloride paste

Four slices each 2-mm were cut from five specimens in each group to the depth of 8 mm (4 slices with about 1.5 mm) (Fig. 2). The first cylindrical specimens were sliced 76 days after molding and 30 days after contamination with the chloride paste, considering the water content nearly homogeneous. The identical depth slices from the same group were mixed and ground for the test of total chlorides in relation to the mass of paste according to ASTM C 1152-90 [7].

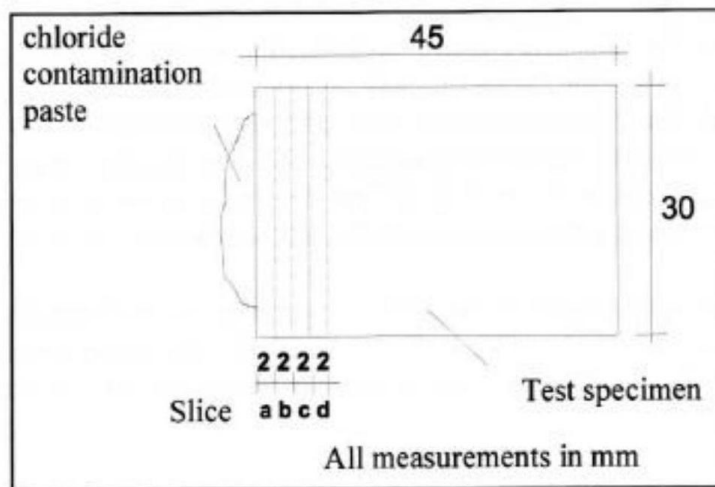


Figure 2. Slicing diagram of test specimens

Tests of free chloride in relation to the cement paste were also performed in the deepest sliced layers, according to ASTM C 1218-92 [8].

To keep the moisture of each group constant, the remaining cylindrical specimens in each group were placed in vacuum plastic bags. This was the most practical method found to keep and control the moisture within each group. The cylindrical specimens of the each group can be weighed together with the bag often since the weight of the plastic bags is known. Before slicing the cylindrical specimens to obtain the second profile, each sample can be weighed separately. The cylindrical specimens in the plastic bags were placed horizontally along their axis. The cylindrical specimens were rotated every 7 days with the plastic bag to alternate positions. These precautions were taken to ensure that the moisture content inside the cylindrical specimens would be kept as constant as possible. Only the 100% SD group was placed in a glass container as described above (Fig. 1d).

The chloride pastes were dried in an oven at $105\pm 5^{\circ}\text{C}$ for 72 hours and they showed an average mass of 1.6 g with a standard deviation of 0.18g. The silicone rings were allowed to dry naturally and had an average mass of 0.35g and standard deviation of 0.13 g.

The remaining cylindrical specimens were sliced 150 days after molding and 30 days after contamination with the chloride paste. The average values of SD between times T_1 and T_2 found in the tests for Groups I, II, III and IV were 57.2%, 74.8%, 90.2% and 97.7%, respectively.

The confidence interval of the SDs of the cylindrical specimens in Groups I, II, III and IV was calculated from the average mass of the $\Phi 30 \times 45$ -mm cylindrical specimens ($48.3\pm 0.61\text{g}$), the mass of the silicone rings ($0.35\pm 0.06\text{g}$), the mass of the

contamination coats ($1.6 \pm 0.17\text{g}$) and absorption after immersion and boiling ($29.7 \pm 1.21\%$). To calculate SD maximum, the lowest values for the mass of cylindrical specimens, silicone rings, contamination coats and the lowest absorption after immersion were used. To calculate SD minimum, the highest mass values and absorption after immersion were used. A 95% confidence value was thus obtained for SDs within the range of $\pm 9.8\%$.

Fig. 3 shows the profiles of average total chloride content in times T_1 and T_2 in the cylindrical specimens of Groups I, II, III and IV. The tests in the chloride containing paste layer for specimens of Groups I, II, III and IV showed a free chloride content by dry paste mass of 0.93%, 0.79%, 0.49% and 0.36% respectively for T_1 , and 0.68%, 0.53%, 0.28% and 0.19% for T_2 .

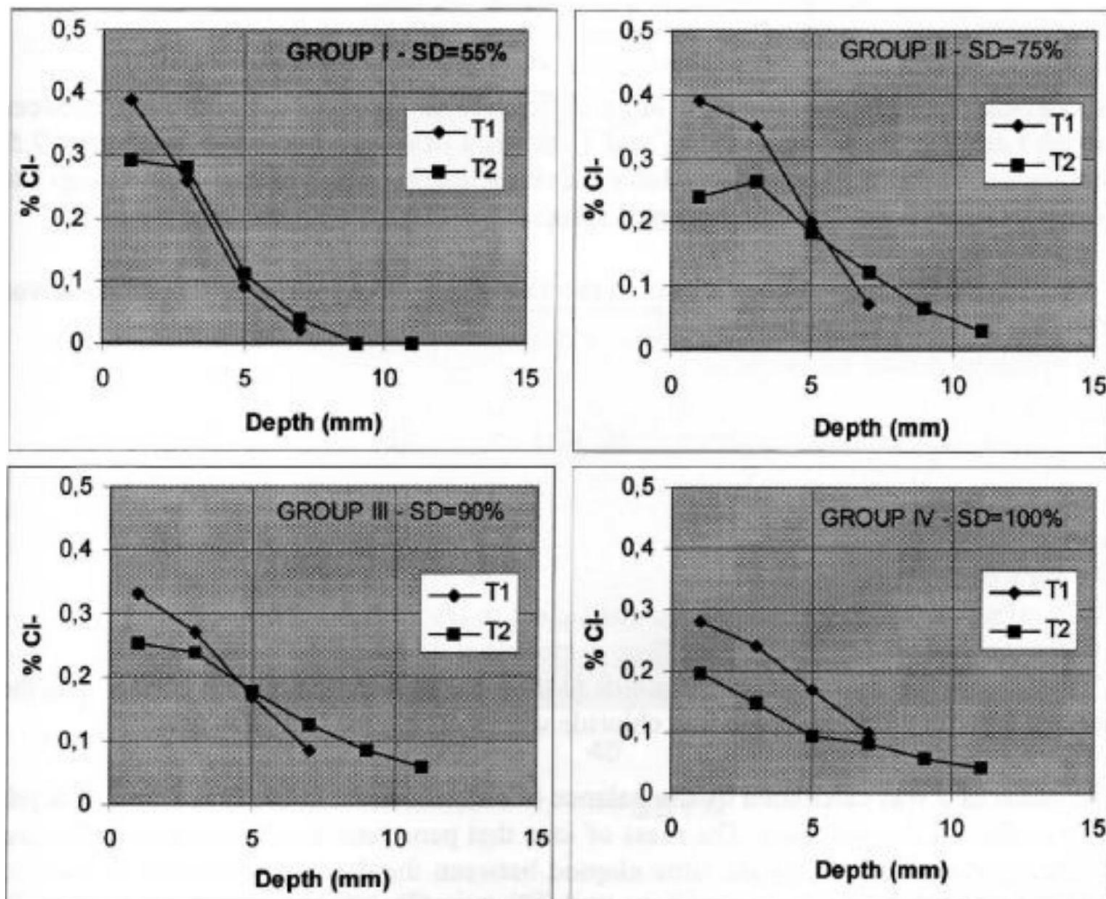


Figure 3. Total chloride profiles: T_1 - cylindrical specimens after 76 days of age and 30 days of contamination; T_2 - cylindrical specimens after 150 days of age and 104 days of contamination

The free chloride content in the fourth sample layer of the cylindrical specimens is 0.02%, 0.05%, 0.02% and 0.07% for Group I, II, III and IV at T_1 , and 0.05%, 0.11%, 0.09% and 0.06% for T_2 , respectively.

2.3. Evaluation of results

Each group showed variations in free chloride content of the contamination layer during the test, and a different average value. This can be attributed to different moisture contents in each group.

By analyzing the T_1 profiles in Fig. 3 and the concentrations of chloride paste contamination layer for each corresponding cylindrical specimens group at T_1 , it can be seen that ion diffusion was more intense than ion penetration by capillary absorption. It follows that chlorides had penetrated less deeply in those cylindrical specimens with smaller SDs, although these that must have a bigger capillary absorption.

A qualitative evaluation shows a large difference in chloride concentration between Group I and Group IV, since the T_1 and T_2 profiles of Group I nearly overlap after 7.5-mm depths. It can also be observed that curve inclinations are reduced from Group I to Group IV. This is evidence of increased chloride penetration with the increase in SD.

To evaluate the diffusion coefficients in the four groups, the following equation derived from the first Fick's Law was used:

$$J = \frac{D_{ef}}{l} (C_1 - C_2) \quad (1)$$

where:

J = flow of chloride ions in $\text{g} \cdot \text{cm}^{-2} \cdot \text{s}^{-1}$,

D_{ef} = effective chloride ion diffusion coefficient in $\text{cm}^2 \cdot \text{s}^{-1}$,

l = thickness of the layer where the flow is measured, in cm, and

C_1 and C_2 are the chloride concentrations in the pore solution on the top surface and the deepest layer in g/cm^3 (average free chloride values during the test were used).

The value of J was calculated by the balance of chloride mass in the first 8 mm of depth of the cylindrical specimens. The mass of ions that penetrate this thickness was divided by the cross-section and by the time elapsed between the data measurement in the first profile (T_1) and the data measurement in the last profile (T_2). The chloride mass at T_1 and T_2 was calculated as a function of the average masses of the chloride contamination paste and the cylindrical specimens layers (assumed to be 2-mm thick, and specific mass determined by tests), and the chloride content measured in each layer (average values for these slices).

The mean concentration of the free chloride solution in the chloride contamination paste (C1) was calculated as a function of the moisture content measured between T1 and T2 and the mass of free chloride at T1 and T2. Two values were obtained and a mean value was calculated. The mean concentration of the solution in the slice between 6 and 8 mm was calculated in the same way.

The value of D_{ef} was calculated with the values of J , l , C_1 and C_2 . These results are presented in a Fig. 4.

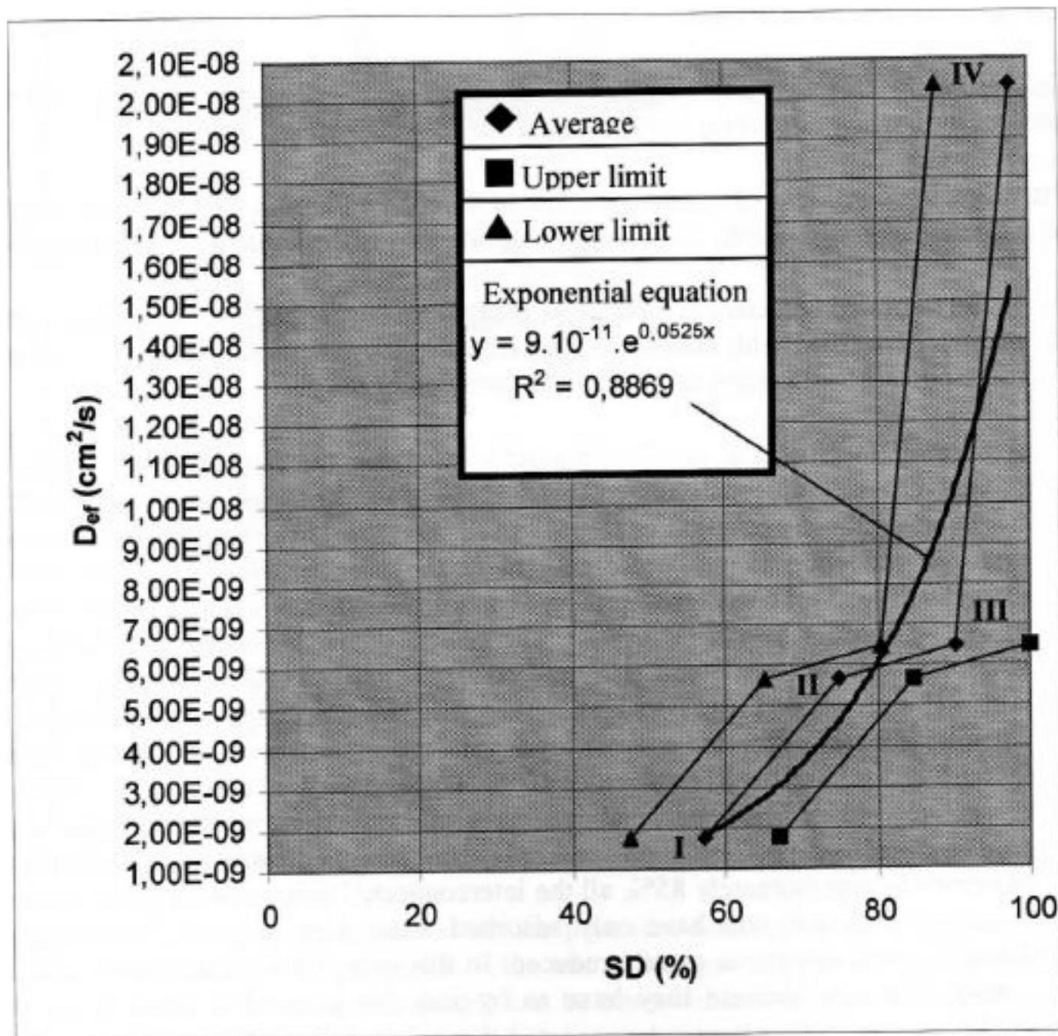


Figure 4. Mean values of the effective diffusion coefficient as a function of SD and the confidence interval of SD average (95% confidence level)

In this figure the results are represented by an exponential equation and show the zone where a variation of SD values can take place. It can be observed that the values of the diffusion coefficient obtained from the average curve are slightly larger than those of the

exponential curve for SDs below 80 %. The difference in the diffusion coefficient derived from the mean curve and the lowest threshold is small for SD values below 85%, with the mean curve values being the lowest.

The ratio between the largest diffusion coefficient (Group IV) and the other values is 0.09 for Group I, 0.28 for Group II and 0.32 for Group III. These ratios show very marked differences, and indicate that the concrete SD is a factor that should be taken into account when analyzing ion diffusion.

2.4. Interpretation of results

The results of this test demonstrate the importance of taking the concrete SD into consideration when estimating the chloride diffusion coefficient.

The following considerations are an attempt to describe a possible mechanism to explain the influence of the SD in the diffusion of chloride ions in the hardened cement paste.

- In the saturated hardened cement paste (Fig. 5) all pores with sizes above the critical diameter are filled with water and this facilitates ion diffusion. The cross-section of these pores is sufficiently large to allow diffusion of ion;
- According to MEHTA and MANMOHAN [9] the number of pores above the critical diameter represents approximately 15% of the voids for cement pastes with a 0.5 w/cm. Thus, a reduction of the SD from 100% to 85% should produce a more dramatic reduction in the water content in the pore network above the critical diameter (Fig. 5). So the cross-section of ion diffusion falls sharply, as can be seen in Fig. 4, between points IV and III. The critical diameter for the paste with a 0.5 w/cm is approximately 80nm [10], and condensation in pores of this size happens with RH above 95% [10]. Therefore, if RH falls below 95%, these pores tend to be filled with water vapor and a water layer with a thickness of approximately 0.2nm, 0.45nm and 0.9nm for RH values of 10%, 50% and 90% is adsorbed on its walls, respectively [11]. Thus, pores above the critical diameter tend to reduce water condensation to the point that only a thin layer of adsorbed water remains. When the SD drops to approximately 85%, all the interconnected pore network (pore diameter > critical diameter) will have only adsorbed water films (Fig. 5). Thus, the ion diffusion cross-section is greatly reduced. In this case, the ions also have to travel greater distances because they have to by-pass the pores. For small water film thicknesses ($\leq 0.9\text{nm}$) it must be expected that precipitates such as Ca(OH)_2 will act as obstacles that block the passage of chloride ions (chloride ion diameter is 0,36 nm);
- For SD below 85 %, the diffusion coefficient should drop less dramatically. This probably happens because water loss begins in the pores that are smaller than the critical diameter, which in turn do not affect mass transport significantly. This is

expected to occur up to the moment when the thickness of the adsorbed water layer in the walls of the pores above the critical diameter starts to decrease, as shown in Fig. 4 between points III and II;

- The diffusion coefficient should again drop sharply (Fig. 4, between points II and I) when the thickness of the water layer adsorbed on the walls of the pores above the critical diameter begins to decrease (Fig. 5).

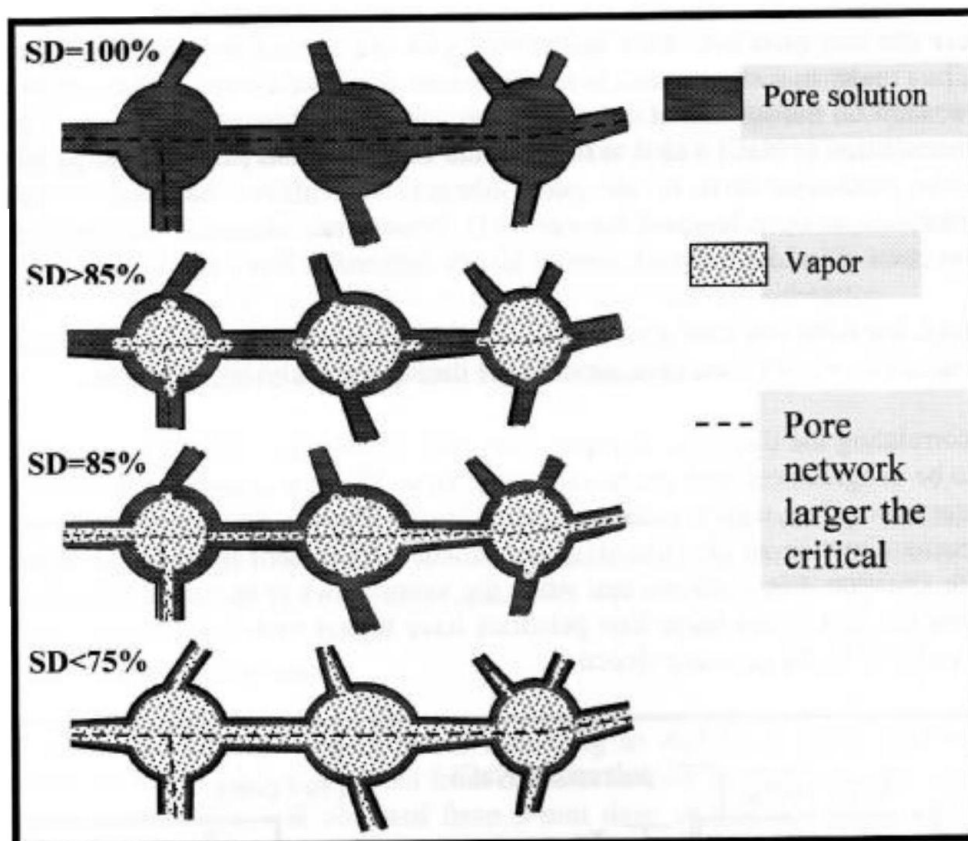


Figure 5. Pore network in hardened cement paste with different moisture contents

This process is very likely to occur when the pore size distribution curve in the cement paste is compared [9] with the results of the test of influence of the moisture content in chloride diffusion in the cement paste. It can be observed that the inflection in the pore size distribution curve in the paste with a 0.6 w/cm occurs when they are filled with mercury to approximately 15% of the pore volume (pore volume above the critical diameter), which is equivalent to a SD of 85% (Fig. 4, between points II and III).

Therefore, it seems wiser to use the average curve according to Fig. 4 than using an exponential correlation, particularly for SDs below 80 %, where higher diffusion coefficients are found in the average curve.

A steady-state flow of chloride ions was assumed when determining the diffusion coefficients in this study and taking into consideration the mean values between the profiles at times T_1 and T_2 on the surface of the cylindrical specimens and in the fourth layer.

To make the determination of the diffusion coefficient according to Second Fick's Law easier, i.e., under non steady-state flow conditions, the chloride ion concentration can be kept constant on the surface of the cylindrical specimens throughout the test. To do so, the concentration of NaCl added to the chloride contamination paste should be increased above the saturation level of the pore solution. This allows water-soluble chloride concentrations to be calculated for each SD, because as dissolved chlorides undergo diffusion, new chlorides that had been so far precipitated as NaCl are dissolved.

Therefore, the diffusion coefficients thus calculated will show some divergence that can be explained by the final considerations made during the analysis of this test.

Tests correlating the direction of vapor flow with the chloride diffusion coefficient [12] seem to be in agreement with the results found here. These tests correlate the direction of the water vapor flow with the diffusion coefficient, showing that when the vapor flows in the same direction as the chlorides, the diffusion coefficient is far bigger than in the opposite situation. Fig. 6 shows that when the vapor flows in the same direction as the chlorides, the first layers these ions penetrate have higher moisture contents than when the vapor flows in the opposite direction.

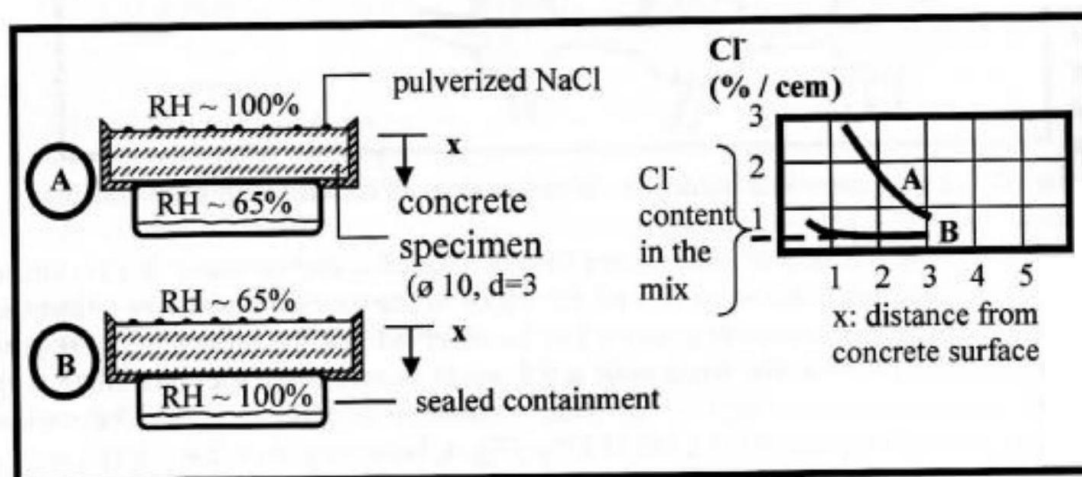


Figure 6. Test correlating the direction of the water vapor flow with the diffusion coefficient [13]

HEDENBLAND [13] theoretically demonstrated the influence of the moisture content in chloride diffusion, showing that the cement hydration degree has a greater influence than the SD. Probably the hydration degree was a little bigger in the groups with higher SDs. However, these groups presented far higher diffusion coefficients, which attested the great influence of SDs. HEDENBLAND [13] had already pointed out that at levels above the SD the precipitation of some elements in the pores of the cement paste could reduce the chloride diffusion coefficient.

MARTYS [14] used computer simulations of ion diffusion in average size pores (interconnected network) filled with two fluids, one fluid is wetting and the second is non-wetting, such as where the water preferentially wets the porous concrete surface and the air. By correlating the SDs of the simulated interconnected pore network with the SDs of the hardened cement paste and using the total pore volume, MARTYS's results show a greater influence of the SD than this paper. However, in the cement paste pores below the critical diameter also affect ion diffusion. Their influence is relatively small when the cement paste is saturated, but when there is little moisture in the interconnected network, the influence of the small pores should be taken into consideration.

3. Concrete structure selected and its characteristics

3.1. Environment

The structural element used in this research was the beam of the vertical surface of the pier of the 'Terminal of Containers-TECON', located in a mist zone. The pier is located in the marine harbor in the city of Rio Grande - RS – Brazil.

3.2. Concrete characteristics

Drilled cores of concrete were extracted according to ASTM C 42-94 [15] and they underwent characterization tests. Data from construction site reports were also used. The chloride content profile was obtained from 5-mm deep drilled out samples (20 holes were made in each of the six points selected in a 50-m section of the 300-m pier). The concrete in this structure was prepared with coarse crushed granite aggregate (maximum diameter - D_{max} - 38 mm) and quartz sand. Pozzolanic cement was used with 34% pozzolan and the cement content was 403 kg/m³. The w/cm was 0.44 with $f_{ck, real} = 23.4$ MPa (28-day strength). The concrete had a specific mass of 2275 kg/m³ and its absorption after immersion and boiling [16] was 5.28% by mass with $f_{ck, real} = 41,0$ MPa (22 years strength). The chloride penetration profile displayed a penetration coefficient (K) for these ions in the order of 5.437 mm · yr^{-1/2} in the model $c_{Cl^-} = K \cdot t^{1/2}$ for a chloride concentration of 0.4 % in relation to the cement content in the boundaries of the attack front.

4. Field test of seasonal variation of the saturation degree in the mist zone

4.1. Test

Drilled cores were extracted from the vertical surface of the TECON pier, and care was taken to remove and discard the outermost layer. The drilled cores thus obtained measured 9.4cm diameter and had the following dimensions: 3 cylindrical specimens with 4cm length and 3 cylindrical specimens with 8cm length. Some cylindrical specimens had their outer surface coated with silicone, with the exception of the top surface (Fig. 7b).

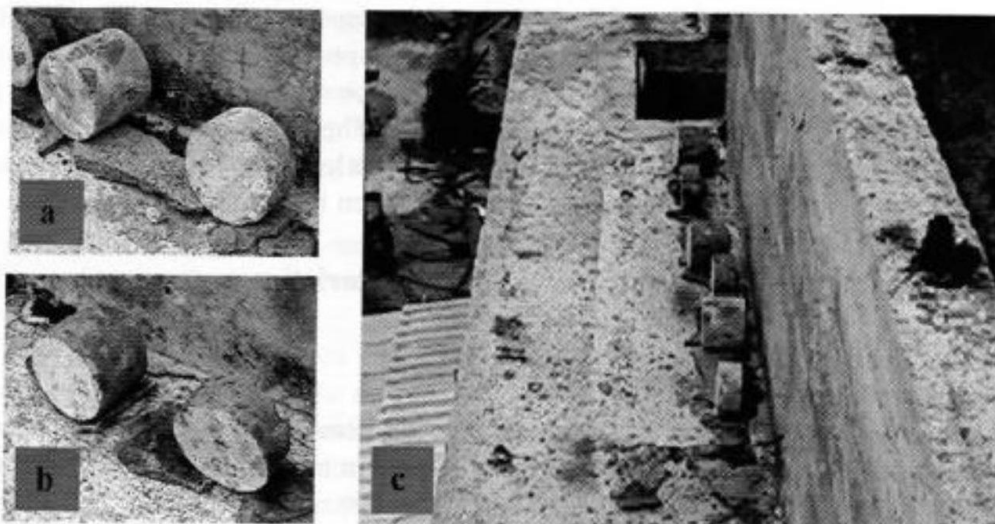


Figure 7. Drilled test specimens - a) not coated; b) coated with silicone; c) with vertical surface displayed in the same position of the vertical surface of the pier

In order to compare the variation of moisture contents in the mist zone, the cylindrical specimens were placed in a structure mounted assembled approximately 10m above the pier surface and 120m from the vertical pier wall. The cylindrical specimens coated with silicone were placed so that the uncoated surface would sit upright, corresponding to the same position of the pier. The cylindrical specimens faced a concrete beam, and were exposed to the same degree of solar irradiation of the upright surface of the pier (Fig. 7c). To prevent flooding by rainwater, the cylindrical specimens were placed on wedges in a place with good drainage conditions.

These precautions were taken to simulate the environmental conditions faced by the vertical surfaces of the pier in the mist zone, and to facilitate access to the cylindrical specimens, which had to be weighed daily in certain periods.

To find out when the cylindrical specimens were in equilibrium with the environment, high moisture and low moisture content cylindrical specimens were placed in the

exposure site. When two cylindrical specimens of the same size and different moisture contents showed a similar behavior, i.e. displayed similar moisture contents and variations, these were deemed to be in equilibrium with the environment. The daily mass of the cylindrical specimens was always taken at the same time, i.e. at 9:00 am.

After measurements were taken in March/1998 (summer measurements), tests of absorption by immersion after boiling (16) were carried out in the cylindrical specimens. After these tests, the 4cm length cylindrical specimens were coated with silicone as described above and placed again in the exposure site. One of the cylindrical specimens had a high moisture content, the second an average moisture content and the third a low moisture content. Winter measurements were thus taken.

4.2. Evaluation of results

Some observations were made after analyzing the daily values of the cylindrical specimens.

The cylindrical specimens that had not been coated with silicone behaved differently from the coated specimens: the increase or the loss in mass was faster both in the 4-cm length and in the 8-cm length cylindrical specimens.

The 4-cm length cylindrical specimens coated with silicone behaved in a similar way after approximately two months of exposure (between the spring and summer of 1999). After the test of absorption by immersion and new exposure to the environment, a similar behavior among cylindrical specimens was observed after approximately one month of exposure (July/1999). Therefore, in the rainy season a similar behavior is observed in a much shorter period of time.

The 8-cm length cylindrical specimens coated with silicone did not reach an equilibrium of moisture with the environment and therefore were not used to analyze results.

4.3. Interpretation of the results

Summer measurements show that the SD remains constant, with an average measured value of approximately 70% and a standard deviation of 1.49%. This corresponds to a variation coefficient of 2.2%. Therefore, SD variation in this season is low.

Winter measurements show an average SD of 85%, with a standard deviation of 4.5% and a variation coefficient of 5.3%. The standard deviation is larger in winter than in summer, but it is still low. This is due to the more frequent rains in winter, which are interspersed with dry periods, when concrete with higher SDs shows faster drying.

5. Applicability of the results

The factors that affect the penetration of chloride ions are applied on the following equations developed from the second Fick's Law:

$$c_{Cl} = 2 (z) (D_{const.Cl^-} \cdot t)^{1/2} \quad (2)$$

where

c_{Cl^-} = thickness in cm,

$D_{const.Cl^-}$ = diffusion coefficient for concrete, considered constant, in cm^2/yr ,

t = service life, in years, and

z = value of the Gauss error function.

$$erf(z) = 1 - (Cc_{Cl} - C_0) / (C_s - C_0) \quad (3)$$

where

Cc_{Cl} = chloride concentration at depth c_{Cl^-} , time t ,

C_0 = initial chloride concentration in the inner part of the structural component concrete,

C_s = chloride concentration in the surface of the structural element, considered constant, and

$erf(z)$ = Gauss error function.

The problem with this model is knowing the precise value of $D_{const.Cl^-}$ for the given conditions of any concrete sample of the structural element in its natural environment under study.

Mist zone

This model was applied to the vertical surface of the beam at the TECON pier, which is located in mist zone.

The effective diffusion coefficient is obtained by comparing the value of the compressive strength of the concrete with values found in the literature, as we explain below.

Because of the large increase in compressive strength in the first two years of service life of any concrete prepared with fly ash additions, two compressive strength values were selected: an average value for the two first years and the practically constant value for the remaining 20 years, which corresponds to 22 years of age of the structure under study.

For the first two years, a characteristic strength $f_{ck, 28 \text{ days}}$ of 23.4 MPa was used. An increase of 67% in two years was found [17], and this is equivalent to an average

compressive strength of 31.2MPa. For the 20 remaining years the compressive strength is 39.1MPa. According to an model proposed by HELENE [18], the diffusion coefficient believed constant ($D_{\text{const.Cl}^-}$) for a concrete with f_{ck} of 30MPa and 40MPa is $316 \cdot 10^{-10} \text{ cm}^2 \cdot \text{s}^{-1}$ and $600 \cdot 10^{-10} \text{ cm}^2 \cdot \text{s}^{-1}$ respectively, for C_s values of 1.2%, C_o values of 0.02% and C_{eCl} values of 0.3%. A mean of $342 \cdot 10^{-10} \text{ cm}^2 \cdot \text{s}^{-1}$ is thus obtained. This value approximates the value found by PAGE et al. [2] for a 0.4 w/cm with normal portland cement (equivalent $f_{\text{ck}} = 30\text{MPa}$) and a temperature of 22.5°C , considering $D_{\text{const.Cl}^-} = D_{\text{ef}}/p$, with porosity p between 0.3 and 0.4 [19] and $D_{\text{ef}} = 227 \cdot 10^{-10} \text{ cm}^2 \cdot \text{s}^{-1}$. The values found by HELENE [18] are very close to the values given in another paper by the same author [20], the values for the effective diffusion coefficient in high resistance concrete are quite similar to those found by GJØRV et al. [5] in laboratory tests, with cylindrical specimens immersed in seawater at an average temperature of 20°C . For the equations above, HELENE's values [18], a temperature of 22.5°C and normal portland cement concrete are considered.

According to ISAIA and HELENE [21] and HELENE's model [18], concrete cover thickness for the reinforcement could be reduced by 20% for concrete prepared with an addition of at least 8% microsilica or 50% of fly ash. For $c_{\text{cl}^-} = K D^{1/2}$, it is equivalent to a 36% reduction in the diffusion coefficient, or a *reduction coefficient of the diffusion coefficient* (R_C) of 0.64.

The influence of temperature is given by the Arrhenius equation:

$$D_T = D_{T_o} e^{-k \left(\frac{1}{T} - \frac{1}{T_o} \right)} \quad (4)$$

where D_T is the effective diffusion coefficient at temperature T , D_{T_o} is the effective diffusion coefficient at temperature T_o , k is the reaction constant, and T and T_o are the temperature ($^\circ\text{K}$).

PAGE et al. [2] carried out tests of the effect of temperature changes on chloride diffusion in paste. Using these data, values of k equal to 5511 and 4766 were found for 0.5 and 0.4 w/cm. A mean value of k was used, and a k_{mean} of 5139 was obtained. For a temperature T_o of 22.5°C and the average temperature in each season, an annual average *reduction coefficient of the diffusion coefficient* was obtained (R_T), as shown in Table 1. Average temperatures were calculated using daily temperature values for the years 1988 to 1998, as supplied by the Fundação Universidade do Rio Grande - National Weather Forecast Institute - 8th District, RS, Brazil.

Table 1. Average values of reduction coefficient of the diffusion coefficient due the variation of the temperature - R_T

$T_0 = 22.5\text{ }^\circ\text{C} = 295.5\text{ K}$				Average
$k = 5139$				
Season	Ti ($^\circ\text{C}$)	Ti(K)	R_T *	0.81
Summer	23.4	296.4	1.05	
Autumn	16.46	289.46	0.70	
Winter	14.37	287.37	0.61	
Spring	20.33	293.33	0.88	

$$* R_T = e^{-k\left(\frac{1}{T} - \frac{1}{T_0}\right)}$$

The reduction coefficient for the diffusion coefficient due the variation of the SD (R_{SD}) was calculated for the average line of Fig. 4 for average SDs measured during the winter and summer. SDs in spring and autumn were considered as being the average value between the winter and summer SDs. These results are presented in Table 2.

Table 2. average values of reduction coefficient of the diffusion coefficient due the variation of the SD - R_{SD}

Season	GS average - %	R_{GS}	R_{GS} average
Summer	70.0	0.226	0.276
Autumn	77.5	0.286	
Winter	85.0	0.305	
Spring	77.5	0.286	

GUIMARÃES et al. [22] studied the effect of the position of the surface in relation to position of concrete molding. It related results on cylindrical specimens whose attacked surface is the lateral surface in relation to the surface of concrete molding (HL) to those whose attack surface is cut from the core of the cylindrical specimens (HC) (Fig. 8) obtained in tests of measurement of the charge passed according to ASTM 1202-94 [23] for cylindrical specimens prepared with concrete with abatement of the conical trunk of 10 cm.

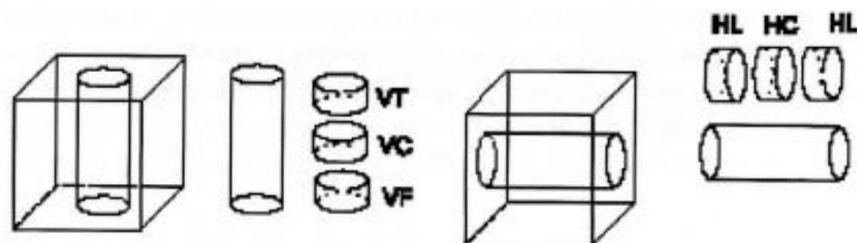


Figure 8. Samples extraction position [22]

The concrete researched is placed in the lateral surface in relation to the surface of concrete molding and this concrete was an abatement of the conical trunk of 8 ± 1 cm. The *reduction coefficient* due to the difference in the position of the extracted lateral surfaces "HL" and within central position with two inner surfaces "HC" (Fig. 8) (R_{SC}) was calculated with the mean of 4 values of charge passed with a resulting R_{SC} of 0,74.

The effective diffusion coefficient was thus calculated considering the conditions of the concrete of the structural element studied in its environment and the type of cement used as a function of the diffusion coefficient found in laboratory tests for concrete prepared with Portland cement:

$$D_{\text{const.Cl}^- \text{ (ef)}} = D_{\text{const.Cl}^- \text{ (lab.)}} R_C R_T R_{SD} R_{SC} \quad (5)$$

Thus, $D_{\text{const.Cl}^- \text{ (ef)}} = 342 \cdot 10^{-10} \text{ cm}^2 \cdot \text{s}^{-1} \cdot 0.64 \cdot 0.81 \cdot 0.276 \cdot 0.74 = 36.2 \cdot 10^{-10} \text{ cm}^2 \cdot \text{s}^{-1}$

The value of z must be found (value of the Gauss error function) before finding the value of the depth of the chloride attack front, according to Eq. 3.

Chloride content in relation to cement mass was considered to be $C_{eCl} = 0.4$ % and $C_o = 0.02$ %.

The value of C_s was calculated according to measurements of chloride content in the first 5 mm of depth. This value corresponds to 0.53 % of the mass of dry concrete.

In the outermost concrete layer, a reduction of the coarse aggregate content must be taken into account because of the wall effect on the contact surface of the mold [24].

The increase in the coarse aggregate content was believed to vary between 0% of the surface of the concrete element to a maximum content in a section that is positioned halfway the diameter of the smallest piece of coarse aggregate that had a significant percentage contribution in the grain size distribution of coarse aggregates. For the concrete used in the samples studied, the diameter of the smallest coarse aggregate with a significant percentage in the grain size distribution of coarse aggregates was 9.5 mm. Therefore, the maximum coarse aggregate content was reached within a distance of approximately 5 mm and the lowest cement content (403 kg/m^3) was found below this depth.

Considering that the outer surface of the concrete is only mortar, we had a specific mass of 2177 kg/m^3 for fresh concrete and 2068 kg/m^3 for dry concrete, and a cement content of 707 kg/m^3 . For a linear reduction of cement content in the external surface to the depth of 5mm, the average of cement content for the first extraction layer (5-mm deep) is 555 kg/m^3 . The mean specific dry mass in this layer was 2171 kg/m^3 , and the value of C_s in the beam of the vertical surface of pier (mist zone) was:

$$C_s = 0,53 \cdot (2171/555)\% = 2.17\% \text{ (in relation to the mass of cement)}$$

With these values we have $\text{erf}(z) = 0.8146$, which corresponds to $z = 0.94$. Thus, we have a model for the mist zone in the environment studied:

$$e_{Cl} = 2 \cdot (0.94) \cdot (36.2 \cdot 10^{-10} \text{ cm}^2 \cdot \text{s}^{-1} \cdot \text{t})^{1/2}$$

$$e_{Cl} = (6.35 \text{ mm} \cdot \text{yr}^{-1/2}) \cdot (\text{t})^{1/2}$$

It can be observed that the value of $6.35 \text{ mm} \cdot \text{yr}^{-1/2}$ corresponds to the coefficient of penetration of chloride ions, and that for the same point the coefficient of penetration of chloride ions calculated from the profile of chloride ions is $5.437 \text{ mm} \cdot \text{yr}^{-1/2}$. The values show a difference of only 17%. If the SD variation (R_{SD}) and the position of the surface exposed in relation the surface of concrete molding (R_{SC}) are not considered, this difference reaches 158%, and the chloride penetration coefficient would be $14.05 \text{ mm} \cdot \text{yr}^{-1/2}$ (Fig. 9), with the SD variation (R_{SD}) being the most significant factor. If only the SD variation is not considered, the difference increases from 17% to 122%.

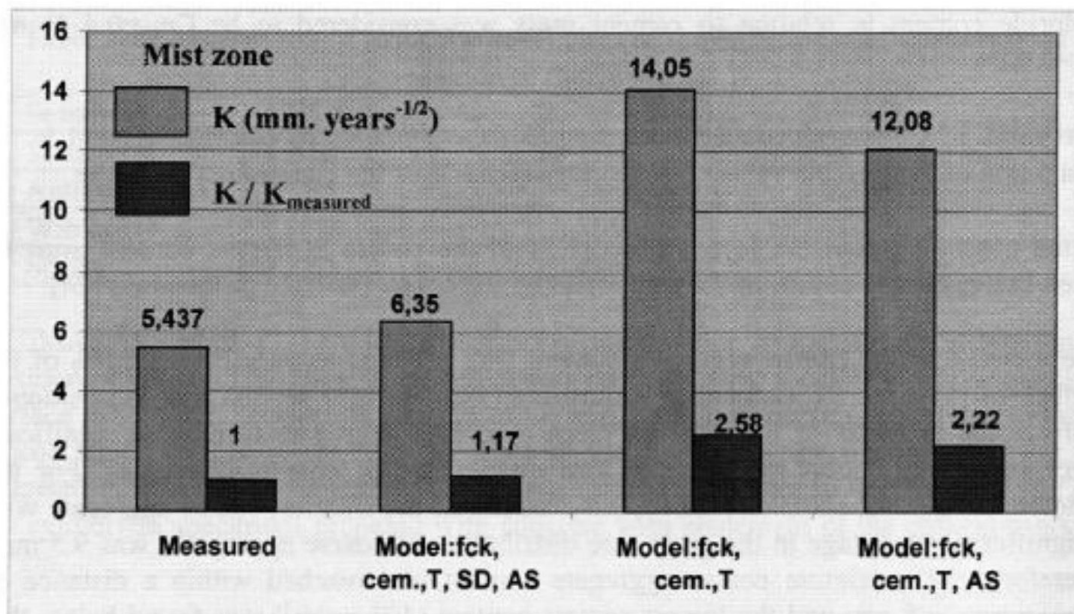


Figure 9. Chloride penetration coefficient - K (mm.yr^{-1/2}) - mist zone from the measured profiles; predicted values considering attack surface (AS) and SD; predicted values not considering attack surface and SD; and predicted values not considering SD

6. Conclusions

The tests carried out in this study and the application of these results in a marine structure indicate a large influence of the SD of the hardened cement paste.

Consequently, this factor must be taken into account when estimating the service life of any reinforced concrete structure under chloride environment. Simpler models can be reviewed including the influence of saturation degree.

7. Acknowledgements

The authors would like to thank the support of FAPESP and FAPERGS (the offices of support to research in Brazil) and the IPT.

8. References

1. Guimarães, A.T.C., 'Desempenho do concreto em ambiente marítimo na região do extremo sul do Brasil'. [Behaviour of Concrete in a Maritime Environment in the South of Brazil] Rio Grande, 1997. Dissertação (Mestrado), Fundação Universidade do Rio Grande, Engenharia Oceânica.
2. Page, C.L., Short, N. R., El Tarras, A., 'Diffusion of chloride ions in hardened cement pastes', *Cem Concr Res* 11 (1981) 395-406.
3. Prudêncio Jr, L. R., 'Durabilidade de concreto frente ao ataque de cloretos e sulfatos'. [Concrete Resistance to Chloride and Sulfate Attack], In: *Qualidade e Durabilidade das Estruturas de Concreto*, Seminário NORIE-UFRS, Porto Alegre, 1993. Anais. 1-12.
4. Andrade, M. C., 'Calculation of chloride diffusion coefficients in concrete from ionic migration measurements', *Cem Concr Res* 23 (1993) 724-742.
5. Gjorv, O. E., Tan, K., Zhang, M., 'Diffusivity of chlorides from seawater into high-strength lightweight concrete', *ACI Materials Journal* 91 (1994) 447-452.
6. American Society for Testing of Materials. Standard specification for Portland Cement - ASTM C 150 - 95. In: *Annual Book of ASTM Standard*. Philadelphia, 1996.
7. Standard test method for acid-soluble chloride in mortar and concrete - ASTM C 1152-90. In: *Annual Book of ASTM Standard*. Philadelphia, 1990.
8. Standard test method for water-soluble chloride in mortar and concrete - ASTM C 1218-92. In: *Annual Book of ASTM Standard*. Philadelphia, 1993.
9. Mehta, P. K., Manmohan, D., 'Pore size distribution and permeability of hardened cement paste', in '7th International Congress on the Chemistry of Cement', *Proceedings of International Congress*, Paris, 1980, Vol. III.
10. Quénard, D., Sallée, H., 'Water vapour adsorption and transfer in cement-base materials: a network simulation', *Materials and Structures* 25 (1992) 515-522.
11. Quénard, D., Sallée, H., 'Le transfert isotherme de la vapeur d'eau condensable dans les matériaux microporeux du bâtiment'. *Cahiers du CSTB*. Livraison 323, Cahier 2525, Oct. 1991.
12. Mehta, P. K., Schiessl, P., Raupach, M., 'Performance and Durability of Concrete Systems', in 'International Congress on the Chemistry of Cement, 9' *Proceedings of International Congress*, New Delhi, Nov. 1992.

Third RILEM workshop on Testing and Modelling the Chloride Ingress into Concrete
9-10 September 2002, Madrid, Spain

13. Hedenbland, G., 'Influence of moisture and carbonation on the transport of chlorides in concrete - some ideas', in 'Corrosion of Reinforcement - Field and Laboratory Studies for Modelling and Service Life', Proceedings, Lund, feb/1995, p. 227-37.
14. Martys, N. S., 'Diffusion in partially-saturated porous materials'. *Materials and Structures* 32 (1999) 555-62.
15. American Society for Testing of Materials. Standard test method for obtaining and testing drilled cores and sawed beams of concrete - ASTM C 42-94. In: *Annual Book of ASTM Standard*. Philadelphia, 1994.
16. Standard test method for specific gravity, absorption, and voids in hardened concrete - ASTM C 642-90. In: *Annual Book of ASTM Standard*. Philadelphia, 1990.
17. Associação Brasileira de Normas Técnicas. Extração, preparo, ensaio e análise de testemunhos de estruturas de concreto - NBR-7680. 1983.
18. Helene, P. R. L., 'Contribuição à normalização: A resistência sob carga mantida e a idade de estimativa da resistência característica; Durabilidade e vida útil das estruturas de concreto armado' [A Contribution to Standardization: Resistance to Sustained Load and Estimated Age of Typical Strength; Durability and Service Life of Reinforced Concrete Structures], São Paulo, 1994. (Monografias. EPUSP).
19. Mehta, P. K., Monteiro, P. J. M., 'Concreto: estrutura, propriedades e materiais' [Concrete: Structures, Properties and Materials] (Pini, São Paulo, 1994).
20. Helene, P. R. L., 'Contribuição ao estudo da corrosão em armaduras de concreto armado' [A Contribution to the Study of Corrosion Processes in Reinforced Concrete Armors], São Paulo, 1993. Tese (Livre Docente), Escola Politécnica da Universidade de São Paulo, Departamento de Engenharia Civil.
21. Isaia, G. C., Helene, P. R. L., 'Durabilidade de concreto de alto desempenho com pozolanas' [Durability of High Performance Pozzolanic Concrete], in 'Seminário Norie-UFRGS : Qualidade e Durabilidade das Estruturas de Concreto', Proceedings, Porto Alegre, 1993, p. 13-33.
22. Guimarães, A. T. C., Tula, L., Helene, P. R. L., 'Performance of surface concrete elements', in 'II International Conference on High-Performance Concrete, and Performance and Quality of Concrete Structures', Proceedings of Conference, Gramado, 1999, CD.
23. American Society for Testing of Materials. Standard test method for electrical indication of concrete's ability to resist chloride ion penetration - ASTM C 1202 -94. In: *Annual Book of ASTM Standard*. Philadelphia, 1994.
24. Coutinho, A. S., 'Fabrico e propriedades do betão' [Concrete Manufacturing and Properties] (Lisboa, Laboratório Nacional de Engenharia Civil, 1973).